

Front matter:

1. Copyright changed to 2009
2. ISBN changed to 978-0-9715292-8-1 (from 978-0-9715292-9-8)

Chapter 1:

1. Figure 1-19a changed to 1-19
2. Figure 1-19b changed to 1-19

Chapter 2:

1. In figures 2-5 and 2-7 the polarity of v_{DS} shown

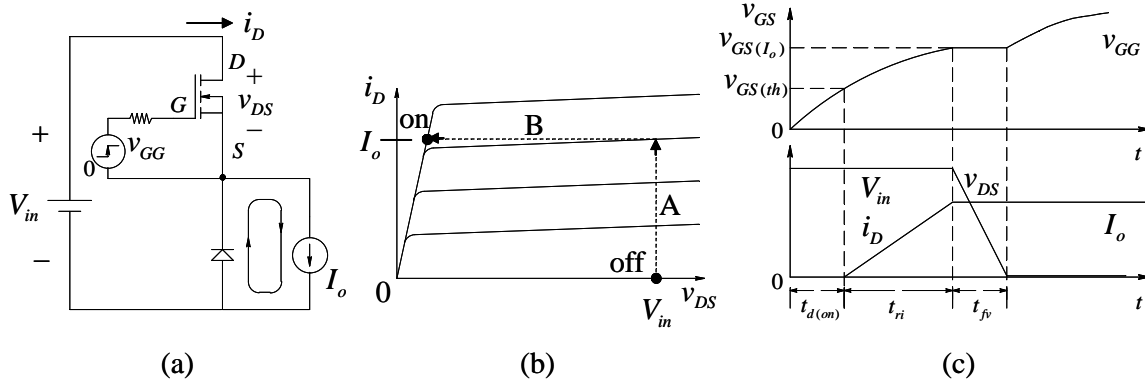


Figure 2-5 MOSFET turn-on.

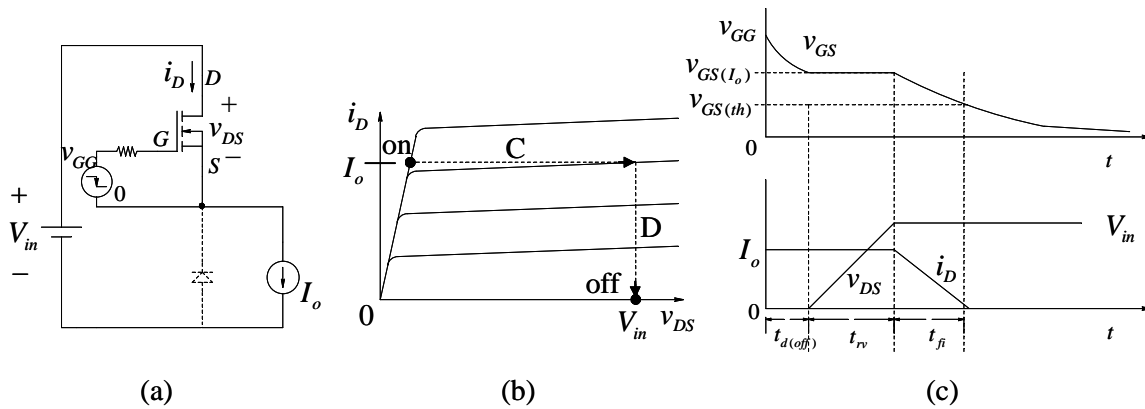


Figure 2-7 MOSFET turn-off.

2. Equation number 2-2 changed to 2-2a
3. Equation number 2-3 changed 2-2b
4. On page 2-19, equation numbers 2A-3 and 2A-4 inserted

$$P_{sw,ideal} = \frac{1}{2} \times V_{in} \times I_o \times (t_{ri} + t_{fv}) \times f_s = 0.6W \quad (2A-3)$$

$$P_{sw,RR} = \frac{1}{2} \times V_{in} \times (I_o + I_{RRM}) \times (t_{ri} + t_{rr}) \times f_s + \frac{1}{2} \times V_{in} \times I_o \times t_{fv} \times f_s = 1.28 W \quad (2A-4)$$

Chapter 3:

1. In figure 3-9, 3.0 micro-seconds changed to 2.917 micro-seconds

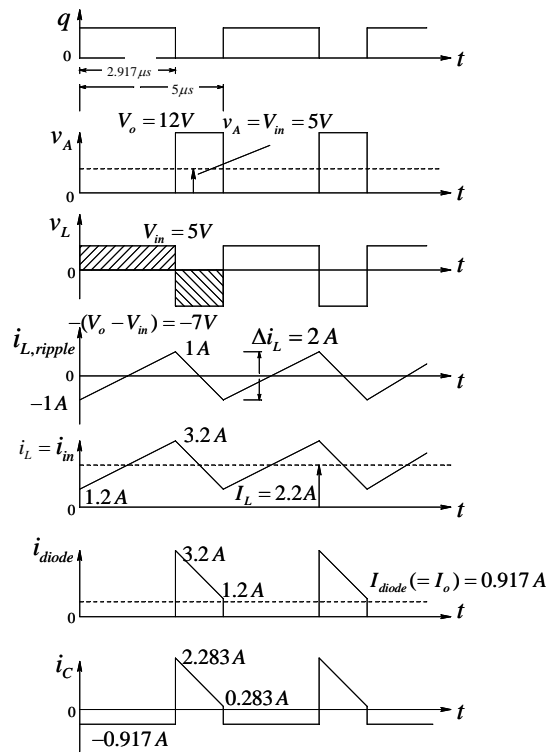


Figure 3-9 Example 3-4.

2. Below equation 3-48b, $R_{crit,D}$ changed to $R_{crit,Buck}$
3. Below equation 3-53b, $R_{crit,D}$ changed to $R_{crit,Boost}$
4. Below equation 3-57, $R_{crit,D}$ changed to $R_{crit,Buck-Boost}$

Chapter 4:

1. In figure 4-2, v_{err} specified

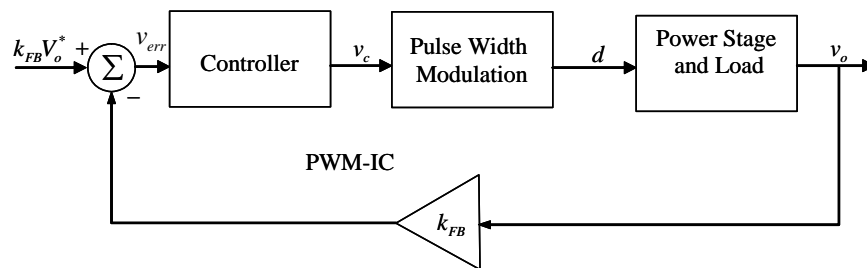


Figure 4-2 Feedback control.

2. Figure 4-12 corrected

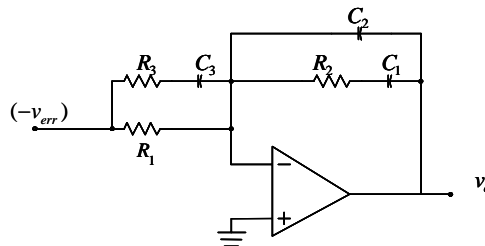


Figure 4-12 Controller implementation of $-G_c(s)$, using Eq. 4-18, by an op-amp.

3. Figure 4-19 corrected

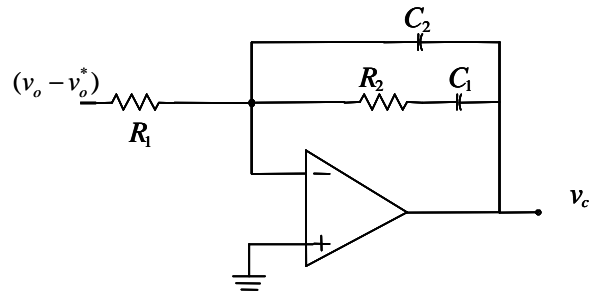


Figure 4-19 Controller implementation of $-G_c(s)$, using Eq. 4-32, by an op-amp.

4. Figure 4-20 corrected

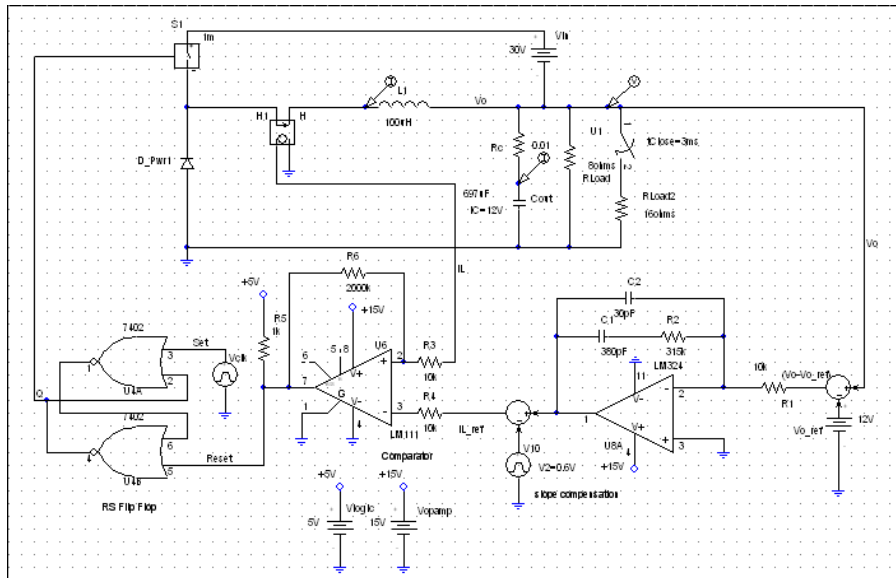


Figure 4-20 PSpice simulation diagram of the peak-current-mode control.

5. Appendix 4-B and 4-C corrected on the CD.

Chapter 6:

1. Figure 6-4 corrected

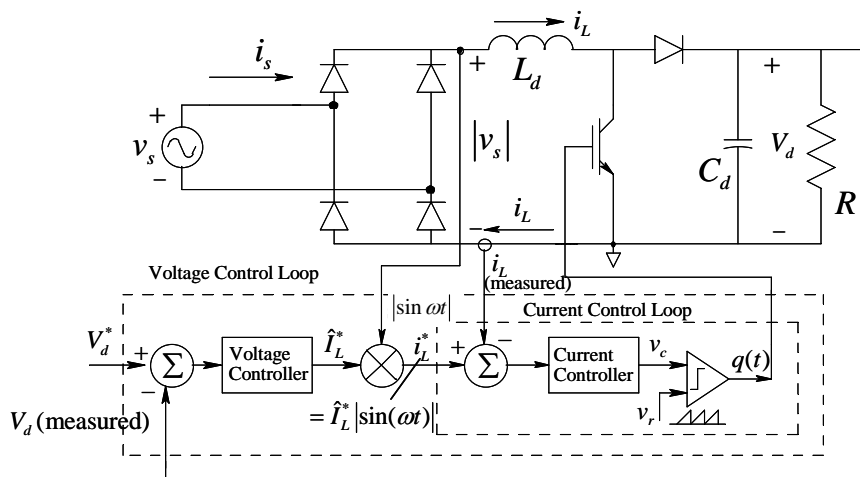


Figure 6-4 PFC control loops.

2. Figure 6-8 corrected

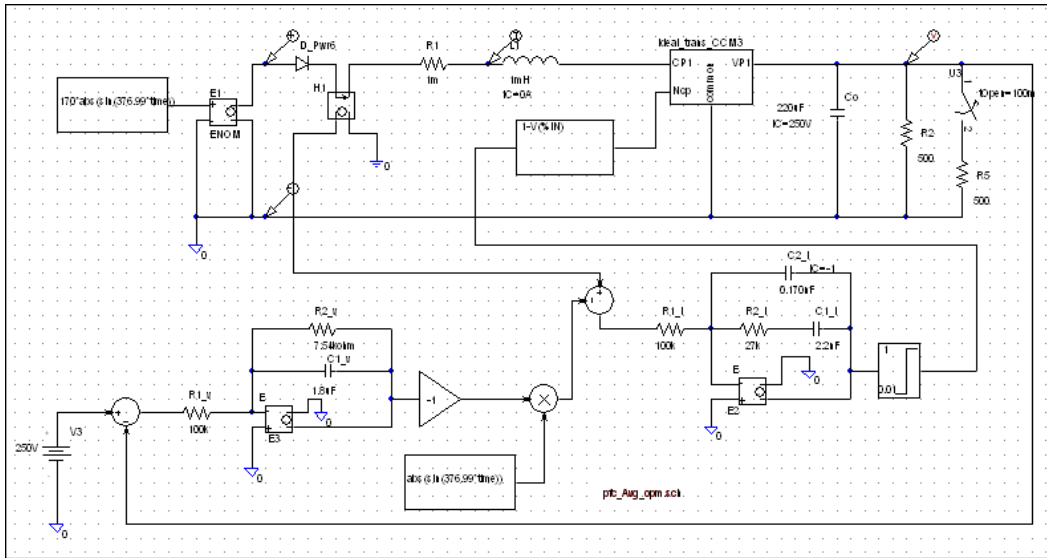


Figure 6-8 PSpice simulation diagram (the load is decreased at 100 ms); for a better resolution, execute the PSpice Schematic on the accompanying CD.

Chapter 13:

- Equation 13-17 changed to 13-17a and equation 13-17b added

$$\Delta V_{\alpha} = \frac{1}{\pi/3} \int_0^{\alpha} \hat{V}_{LL} \sin \omega t \cdot d(\omega t) = \frac{3}{\pi} \hat{V}_{LL} (1 - \cos \alpha) \quad (13-17a)$$

Using Eqs. 13-16 and 13-17a, with a finite delay angle α , the dc-side voltage is

$$V_{d\alpha} = \frac{3}{\pi} \hat{V}_{LL} \cos \alpha = V_{do} \cos \alpha \quad (13-17b)$$

Chapter 14:

- Section 14-4-1 expanded with new figures

14-4-1 Wind-Electric Systems

Wind energy is an indirect manifestation of solar energy, caused by uneven heating of the earth's surface by the sun. Out of all renewable energies, wind has come a long way and still this potential is just beginning to be realized. Fig. 14-8 shows the wind potential by states in the United States, where there are several areas with good to excellent wind conditions.

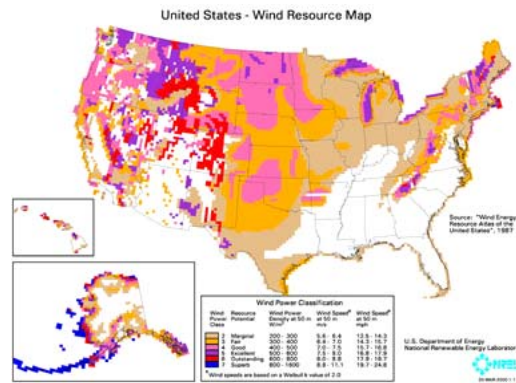


Fig. 14-8 Wind-resource map of the United States.

Commonly used schemes for power generation in windmills require a gearing mechanism because the wind turbine rotates at very slow speeds, whereas the generator operates at a high speed close to the synchronous speed, which at the 60-Hz line frequency would be 1800 rpm for a 4-pole and 900 rpm for an 8-pole machine. Therefore, the nacelle contains a gearing mechanism that boosts up the turbine speed to drive the generator at a higher speed; need for a gearing mechanism is one of the inherent drawbacks of such schemes. There are proposal to use direct-drive (without gears) permanent magnet machines in very large sizes, however in practice, most windmills use gearing. This subsection describes various types of wind-generation schemes.

Induction Generators, Directly Connected to the Grid. As shown in Fig. 14-9a, this is the simplest scheme, where a wind-turbine driven squirrel-cage induction generator is directly connected to the grid through a back-to-back connected thyristor-pair for soft-start. Therefore, it is least expensive and uses a rugged squirrel-cage rotor induction machine.

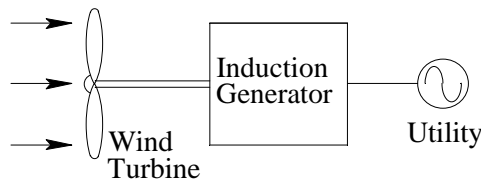


Fig. 14-9a Induction generator directly connected to the grid.

For the induction machine to operate in its generator mode, the rotor speed must be greater than the synchronous speed. The drawback of this scheme is that since the induction machine always operates very close to the synchronous speed, this scheme is not optimum at low and high wind speeds compared to variable speed schemes described below. Another disadvantage of this scheme is that a squirrel-cage induction machine always operates at a lagging power factor (that is, it draws reactive power from the grid as an inductive-load would). Therefore, a separate source, for example shunt-connected capacitors are often needed to supply the reactive power to overcome the lagging power factor operation of the induction machine.

Doubly-Fed, Wound-Rotor Induction Generators. The scheme in Fig. 14-9b utilizes a wound-rotor induction machine where the stator is directly connected to the utility supply and the rotor is injected desired currents through a power-electronics interface. Typically, four-fifth of the power flows directly from the stator to the grid and only one-fifth of the power flows through the power electronics in the rotor circuit. The drawback of this scheme is that it uses a wound-rotor induction machine where the currents to the three-phase wound rotor are supplied through slip-rings and brushes which require maintenance. In spite of the fact that power electronics is expensive, since power electronics is rated only one-fifth of the system rating, therefore the overall cost is not much higher than the previous scheme. However, there are several distinct advantages over the previous scheme, as described below.

The scheme using a doubly-fed wound-rotor induction machine can typically operate in a range $\pm 30\%$ around the synchronous speed and hence it is able to capture more power at lower and higher wind speeds compared to the previous scheme because it can operate at above, as well as below, the synchronous speed. It can also supply reactive power, whereas in the previous scheme, the squirrel-cage induction machine only absorbs reactive power. Therefore, the scheme using a doubly-fed wound-rotor induction machine is quite popular in windmills being installed in the United States.

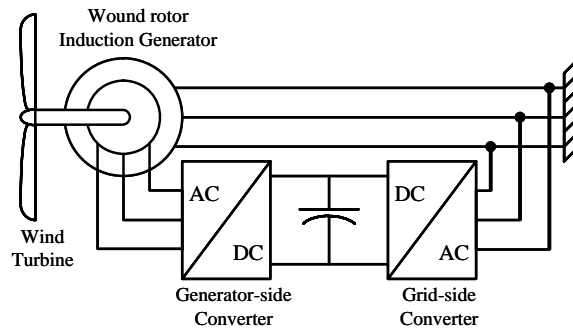


Fig. 14-9b Doubly-fed, wound-rotor induction generator.

Power Electronics Connected Generator. In the third scheme shown in Fig. 14-9c, a squirrel-cage induction generator or a permanent-magnet generator is connected to the grid through a power electronics interface. This interface consists of two converters. The converter at the generator-end supplies the reactive power excitation needed if it is an induction generator. Its frequency of operation is controlled to be optimum for the prevailing wind speed. The converter at the line-end is capable of absorbing or supplying reactive power in a continuous manner. This is the most flexible arrangement using a rugged squirrel-cage machine or a high-efficiency permanent-magnet generator, which can operate in a very wide wind-speed range and is the likely contender for the future arrangements as the cost of the power electronics interface, that must handle the entire power output of the system, is continuing to go down.

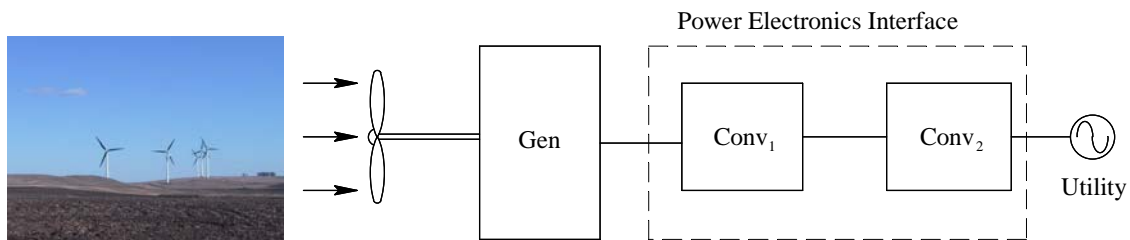


Fig. 14-9c Power Electronics connected generator.

CD-ROM:

1. Presentation slides have been modified to reflect the changes above.
2. PSpice exercises have been modified to reflect the changes above.